

Domain wall junctions as vortices: static structure

H Büttner¹, Yu B Gaididei², Avadh Saxena³, Turab Lookman³
and A R Bishop³

¹ Physikalisches Institut, Universität Bayreuth, Bayreuth D-95440, Germany

² Bogolyubov Institute for Theoretical Physics, Metrologichna Str. 14 B, 01413, Kiev, Ukraine

³ Theoretical Division and Center for Nonlinear Studies, Los Alamos National Laboratory,
Los Alamos, NM 87545, USA

Received 10 March 2004

Published 24 August 2004

Online at stacks.iop.org/JPhysA/37/8595

doi:10.1088/0305-4470/37/36/002

Abstract

For a model system with a complex scalar field static topological solutions are found analytically. Various domain wall structures are discussed and especially the junction of three different domains (called Y-type junctions) is studied in detail. It is shown that these junction structures are equivalent to a vortex with winding number $k = 1$.

PACS numbers: 05.45.-a, 11.27.+d

1. Introduction

In many fields of physics topological defects (domain walls, vortices, strings, etc) are recognized as being fundamentally important for the understanding of the dynamics and thermodynamics (see, e.g., the general references [1–4]). The defects were studied quite early in non-equilibrium systems [5, 6] as well as in field theoretic models, see [7–13]. Topological defects with nontrivial core structure were invoked to explain the cosmological expansion (inflation) [14, 15]. Stability and dynamics of vortices in a dark matter condensate were also studied [16–18]. There are also a large number of investigations of the structure of topological defects in various fields of physics, ranging from phase transitions in the core of defects [19] to domain patterns in ferroelectrics [20] and ferroelastics [21, 22], not to mention several studies on dislocations in pattern forming systems, see the early work in [23]. Some new developments are found in such fields as singular optics [24], Bose–Einstein condensation of dilute atomic gases [25], and magnetic nanostructures [26, 27]. Despite this large number of interesting results, there are only the cases of special sine–Gordon models where single vortices and vortex dipoles were studied by the inverse scattering method [28] and it is discussed that the intersection of domain walls can be consistently described as a vortex structure [29, 30].

The goal of this paper is to investigate topological defects in a two-component field theory with three-fold rotation symmetry. In the model we analyse in this article, stable solutions of this kind have the winding number $k = 1$ and we analytically show that our model has an interesting behaviour near the junction point as well as asymptotically. In section 2 we present the model, derive the Euler–Lagrange equations and discuss the properties of their spatially homogeneous solutions. In section 3 we discuss the basic topological excitations of the system: domain walls and vortices. In subsection 3.1, we study domain walls which link different variant phases and show that the domain boundary between variants is described by a kink-like solution for one component of the field and a pulse-like solution for the other component. In subsection 3.2, we study domain wall junctions when three domain walls meet at one point. We show that this type of excitation is characterized by a topological charge equal to 1 and it may be considered as a vortex or more precisely as a ‘textured vortex’. We study both near-field and far-field configurations. The latter is studied by using a new asymptotic approach within a framework where the radial part of the Laplacian is neglected. In appendix B we develop a collective-coordinate-like method which justifies the accuracy of our approach.

2. Model and Euler–Lagrange equations

We consider a model with a scalar complex field $\phi(\vec{r}) = \phi_1(\vec{r}) + i\phi_2(\vec{r})$ in two space dimensions. The action is defined by

$$S = \int d\vec{r} \left\{ \frac{1}{2} \partial_\alpha \phi \partial_\alpha \phi^* + V(\phi, \phi^*) \right\}. \quad (1)$$

Here $V = V(\phi, \phi^*)$ is the potential which we choose in the form

$$V(\phi, \phi^*) = -\frac{1}{2} \tau |\phi|^2 - \frac{1}{6} (\phi^3 + \phi^{*3}) + \frac{1}{4} |\phi|^4, \quad (2)$$

where $\tau > 0$ is a dimensionless parameter. Action (1) is invariant under operations

$$\phi \rightarrow \phi e^{i\alpha \frac{2\pi}{3}}, \quad \phi^* \rightarrow \phi^* e^{-i\alpha \frac{2\pi}{3}}, \quad \alpha = 0, 1, 2, \dots \quad (3)$$

of the $Z(3)$ group, which is of importance in solid state physics [31] and in non-Abelian gauge theories where it is the centre of the $SU(3)$ group (see, for example, [32, 33]). In the Landau theory of ferroelastic phase transitions, the function (2) represents the elastic free energy of (i) triangle–rectangle transition with ϕ_1 and ϕ_2 being the two components of shear strain [21, 22] or (ii) cubic–tetragonal ferroelastics with ϕ_1 and ϕ_2 being the two components of the deviatoric strain [35, 36]. Note that this corresponds to a homogeneous elastic problem (and thus the elastic compatibility constraint is automatically satisfied and other components of the strain tensor are not involved). However, for the Y-junctions discussed below we have a spatially inhomogeneous structure near the centre and the elastic compatibility constraint cannot be neglected in general. For small bulk modulus materials it is a good approximation to neglect this constraint. Besides, here we are interested in a general discussion of these complex fields and thus we describe an unconstrained model and defer the study of the effect of constraints to a later paper. The dimensionless parameter τ has the meaning of a temperature-dependent elastic constant. Other applications may include QCD where action (1) describes a system which contains only gluons but no other particles [8, 37].

By introducing the current \vec{J} :

$$\vec{J} = (\phi_1 \partial_x \phi_2 - \phi_2 \partial_x \phi_1, \phi_1 \partial_y \phi_2 - \phi_2 \partial_y \phi_1, 0), \quad (4)$$

we may observe that the quantity

$$Q = \int_A dx dy (\partial_x \phi_1 \partial_y \phi_2 - \partial_x \phi_2 \partial_y \phi_1), \quad (5)$$

where A is the area of the system, can be expressed as a circulation around the boundary curve C :

$$Q = \int_A dx dy (\vec{\nabla} \times \vec{J})_z = \frac{1}{2} \oint_C \vec{J} \cdot d\vec{r}. \quad (6)$$

Thus, the quantity Q plays a role of charge and can be considered as a topological invariant.

By using the new variables

$$\phi_1 = \epsilon \cos \Phi, \quad \phi_2 = \epsilon \sin \Phi \quad (7)$$

where $\epsilon = \sqrt{\phi_1^2 + \phi_2^2}$ is the amplitude and $\Phi = \arctan(\phi_2/\phi_1)$ is the phase, the potential function (2) takes the form

$$V = -\frac{\tau}{2} \epsilon^2 - \frac{1}{3} \epsilon^3 \cos(3\Phi) + \frac{1}{4} \epsilon^4. \quad (8)$$

The potential energy has a maximum at

$$\phi_1 = \phi_2 = 0, \quad (9)$$

and three minima which form an equilateral triangle:

$$(\phi_1, \phi_2) = \epsilon_0 (\cos \Phi, \sin \Phi), \quad \epsilon_0 \equiv \frac{1 + \sqrt{1 + 4\tau}}{2}, \quad \Phi = 0, 2\pi/3, 4\pi/3. \quad (10)$$

These three minima represent three vacuum (ground) states which are separated by the three saddle points

$$(\phi_1, \phi_2) = |\epsilon_1| (\cos \Phi, \sin \Phi), \quad \epsilon_1 \equiv \frac{1 - \sqrt{1 + 4\tau}}{2}, \quad \Phi = \pi/3, \pi, 5\pi/3. \quad (11)$$

The spatial structure of the system is determined by the Euler–Lagrange equations

$$\begin{aligned} -\nabla^2 \phi_1 - \tau \phi_1 - \phi_1^2 + \phi_2^2 + (\phi_1^2 + \phi_2^2) \phi_1 &= 0, \\ -\nabla^2 \phi_2 - \tau \phi_2 + 2\phi_1 \phi_2 + (\phi_1^2 + \phi_2^2) \phi_2 &= 0. \end{aligned} \quad (12)$$

Next, we find some specific solutions of these equations.

3. Topological defects

Topologically stable nonlinear excitations in situations with degenerate ground state include domain walls and vortices.

3.1. Domain walls

Let us analyse the domain walls linking two variant phases. We are interested in the solutions which depend on one spatial coordinate x . As was first shown in [34], there is a notable special case here: $\tau = 2$. For this temperature, the saddle point with $\Phi = \pi$ ($\phi_1 = -1, \phi_2 = 0$) lies on the straight line which connects two minima with $\Phi = 2\pi/3$ and $4\pi/3$ ($\phi_1 = -1, \phi_2 = -\sqrt{3}$ and $\phi_1 = -1, \phi_2 = \sqrt{3}$).

For $\tau = 2$ the first of equations (12) has a solution $\phi_1 = -1$ and the equation for ϕ_2 takes the form

$$\partial_x^2 \phi_2 + 3\phi_2 - \phi_2^3 = 0. \quad (13)$$

The solution of equation (13) which satisfies the boundary conditions $\phi_2 \rightarrow \pm\sqrt{3}$ when $x \rightarrow \pm\infty$ has the form of kinks, i.e.

$$\phi_2(x) = \sqrt{3} \tanh\left(\sqrt{\frac{3}{2}}x\right). \quad (14)$$

Another two pairs of domain walls linking two phases may be obtained from equations (13) by rotating the coordinate system through the angles $\pi/3$ and $2\pi/3$.

When the temperature τ deviates from this particular value: $\tau = 2 - \delta$ where $|\delta| < 1$, one can use a perturbation approach based on the fact that for small δ a deviation of the function $\phi_1(x)$ from the constant value is also small.

After lengthy but straightforward calculations (see appendix A for details), we obtain that the domain boundary between two variants in the temperature interval τ : $|2 - \tau| < 1$ is described by a kink-type solution for $\phi_2(x)$ of the form

$$\phi_2(x) = \sqrt{3} \left(1 - \frac{2 - \tau}{6}\right) \tanh\left(\sqrt{\frac{1 + \tau}{2}}x\right), \quad (15)$$

and a pulse-type solution for the component $\phi_1(x)$:

$$\begin{aligned} \phi_1(x) = -1 + \frac{2 - \tau}{9} \left\{ 1 + 2 \cosh^2\left(\sqrt{\frac{1 + \tau}{2}}x\right) \ln\left(2 \cosh\left(\sqrt{\frac{1 + \tau}{2}}x\right)\right) \right. \\ \left. - \sqrt{\frac{1 + \tau}{2}}x \left(1 + 2 \cosh^2\left(\sqrt{\frac{1 + \tau}{2}}x\right)\right) \tanh\left(\sqrt{\frac{1 + \tau}{2}}x\right) \right\}. \quad (16) \end{aligned}$$

The height of the pulse is proportional to the temperature difference $2 - \tau$. For $\tau < 2$ the field ϕ_1 represents a bright soliton while for $\tau > 2$ equation (16) gives a dark soliton. Figure 1 presents the structure of the corresponding $\phi_1(x)$, $\phi_2(x)$ variant–variant domain walls. It is seen that their profiles coincide with the ones obtained in [35, 38] by direct numerical simulations of equations (A1).

3.2. Y-type junctions

In this subsection, we consider the case when three phases coexist. It was shown in [39] that in systems with three equivalent ground states three interfaces can meet, creating a ‘triple junction’ with the angle $2\pi/3$ between them. Given that a stable intersection exists¹, we would like to find an analytic solution to the Euler–Lagrange equations (12) which describes a ‘Y intersection’ or as we rightly term it a ‘textured vortex’. The aim of this subsection is to show that this solution is vortex-like with topological charge equal to 1.

In terms of the polar variables (7) action (1) has the form

$$S = \int d\vec{r} \left\{ \frac{1}{2}((\nabla\epsilon)^2 + \epsilon^2(\nabla\Phi)^2) - \frac{1}{2}\tau\epsilon^2 - \frac{1}{3}\epsilon^3 \cos(3\Phi) + \frac{1}{4}\epsilon^4 \right\}. \quad (17)$$

¹ Preliminary results of our numerical studies of relaxation dynamics of the relevant Landau–Ginzburg model with a two-component order parameter: shear and deviatoric strains in triangular lattices (see [22] for a more detailed description of the model) show that the lattices with very small bulk modulus may evolve to a Y-junction-like structure if a seed with a winding number $k = 1$ is used as an initial configuration.

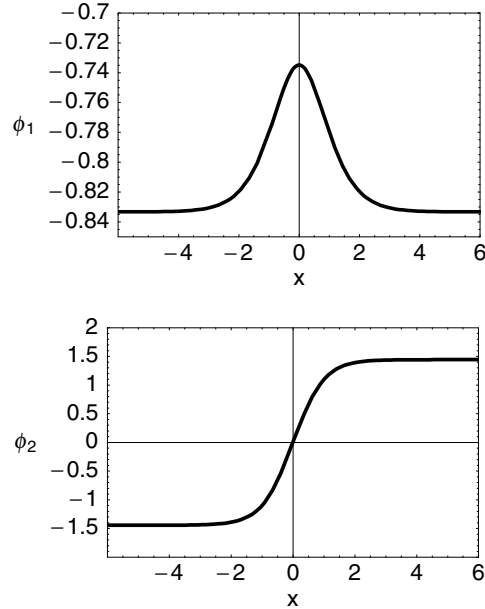


Figure 1. The variation of the real (ϕ_1) and imaginary (ϕ_2) parts of the field in the domain wall linking two variant phases for the special case $\tau = 1$.

Euler–Lagrange equations for the quantities ϵ and Φ are

$$-\nabla^2 \epsilon + \epsilon (\nabla \Phi)^2 - \tau \epsilon - \epsilon^2 \cos(3\Phi) + \epsilon^3 = 0, \quad (18)$$

$$-\nabla(\epsilon^2 \nabla \Phi) + \epsilon^3 \sin(3\Phi) = 0. \quad (19)$$

Vortex-like structures described by equations (18) and (19) are characterized by the non-vanishing value of the invariant (5) which can be written in the form

$$Q = \oint_c \epsilon^2 \nabla \Phi \cdot d\vec{r}, \quad (20)$$

or by the so-called winding number (topological charge) $k = 1, 2, 3, \dots$ which is determined from the condition

$$\int_{\Gamma} (\partial_x \Phi dx + \partial_y \Phi dy) = 2\pi k, \quad (21)$$

where Γ is an arbitrary contour surrounding the centre of the vortex.

It is convenient to use the polar coordinates

$$x = r \cos \chi, \quad y = r \sin \chi. \quad (22)$$

In what follows we restrict ourselves to the case of vortices with $k = 1$. This means that we solve equations (18) and (19) under the boundary conditions

$$\begin{aligned} \epsilon(0, \chi) &= 0, & \epsilon(r, \chi + 2n\pi/3) &= \epsilon(r, \chi), \\ \Phi(r, \chi + 2n\pi/3) &= \Phi(r, \chi) + 2n\pi/3, & n &= 0, 1, 2, \dots \end{aligned} \quad (23)$$

Note that when the third-order nonlinear term in action (1) is absent, equation (18) has a radially symmetric solution $\epsilon(r, \chi) = \epsilon(r)$, while equation (19) has the solution $\Phi(r, \chi) = k\chi$. The

existence of the third-order invariant makes a radially symmetric solution impossible for ϵ and the dependence of ϵ on azimuthal angle χ must be taken into account. It can be achieved by seeking the solutions of equations (18) and (19) in the form of Fourier series

$$\Phi(r, \chi) = \chi + \sum_{j=1}^{\infty} \psi_j(r) \sin(3j\chi), \quad \epsilon(r, \chi) = \sum_{j=0}^{\infty} \epsilon_j(r) \cos(3j\chi). \quad (24)$$

With this Ansatz (24) the boundary conditions (23) are automatically satisfied. Let us consider the near-field distribution, i.e., the behaviour near the centre of the vortex ($x^2 + y^2 \rightarrow 0$). Substituting (24) into equations (18), (19) and restricting our consideration to first terms in the Fourier expansions (24), we find that

$$\Phi(r, \chi) = \chi + \psi_1(r) \sin(3\chi) + \dots, \quad \psi_1(r) = \frac{a_1^2 + 6a_2}{6a_1} r^3 + \mathcal{O}(r^5), \quad (25)$$

$$\epsilon(r) = \epsilon_0(r) + \epsilon_1(r) \cos(3\chi) + \dots, \quad \epsilon_0 = a_1 r - \frac{a_1}{8} \tau r^3 + \mathcal{O}(r^5), \quad (26)$$

$$\epsilon_1(r) = a_2 r^4 + \mathcal{O}(r^6),$$

where all terms r^n ($n \geq 5$) are neglected. The constants a_j ($j = 1, 2$) are determined below by matching the expansion (24) and asymptotic expansion for $r \gg 1$.

The asymptotic behaviour of $\epsilon(r)$ as $r \rightarrow \infty$ or in other words the far-field behaviour may be established from (18) by putting $\nabla\epsilon = 0$ and $\nabla\Phi = 0$, and for $\tau > 1$ to a good approximation it has the form

$$\epsilon(r) = \frac{\cos 3\Phi + \sqrt{4\tau + \cos^2 3\Phi}}{2} \approx \sqrt{\tau} + \frac{1}{2} \cos 3\Phi, \quad (27)$$

$$\left(\partial_r^2 + \frac{1}{r} \partial_r \right) \Phi + \frac{1}{r^2} \partial_\chi^2 \Phi = \sqrt{\tau} \sin 3\Phi. \quad (28)$$

Note that in equation (28) we neglected the term $\sin 6\Phi$ because in the range of parameters under consideration ($\tau > 1$) it does not change the qualitative behaviour of the phase function Φ .²

As a first step let us neglect the radial part of the Laplacian operator (the first two terms in the lhs of equation (28)) and consider the truncated sine-Gordon equation

$$\partial_\chi^2 \Phi = \sqrt{\tau} r^2 \sin 3\Phi. \quad (29)$$

As a result, we obtain

$$\Phi(r, \chi) = -\frac{\pi}{3} + \frac{2}{3} \operatorname{am} \left(\sqrt{\frac{3}{m}} \tau^{1/4} r \chi \middle| m \right). \quad (30)$$

Here $\operatorname{am}(u|m)$ is the Jacobian amplitude elliptic function with modulus m [40]. The modulus m is determined from the boundary conditions (23) by the equation

$$\tau^{1/4} r = \frac{\sqrt{3m}}{\pi} \mathbf{K}(m), \quad (31)$$

² It is interesting to note that the function Φ obtained from the angular part of the two-dimensional sine-Gordon equation (i.e. by neglecting the radial part of the Laplacian operator) describes the angular dependence with very good accuracy. We used this approach for the case of tetragonal systems when the rhs of equation (28) is $\sin 4\Phi$ and for which an exact vortex-like solution with the winding number equal to 1 is known (see, e.g., [43]). Comparing this solution with an approximate one obtained within the framework of the same approach as we used in this paper we found out that for $r \geq 2$ they differ by 0.3%.

and function (30) takes the form

$$\Phi(r, \chi) = -\frac{\pi}{3} + \frac{2}{3} \operatorname{am} \left(\frac{3}{\pi} \chi \mathbf{K}(m) \middle| m \right), \tag{32}$$

where $\mathbf{K}(m)$ is the complete elliptic integral of the first kind [40]. Introducing equation (30) into equation (27) we get

$$\epsilon = \sqrt{\tau} - \frac{1}{2} + sn^2 \left(\sqrt{\frac{3}{m}} \tau^{1/4} r \chi \middle| m \right). \tag{33}$$

To check the accuracy of our approximation we used a collective-variable-like approach (see appendix B for details). As a result we find that for $r > 1$ the inclusion in the analysis of the radial part of Laplace operator leads to the following modification of relation (31):

$$\mathbf{K} \approx \frac{\pi r \tau^{1/4}}{\sqrt{3}} \left(1 + \frac{\pi^2}{36r^2 \tau^{1/2}} \right)^{-1/2}. \tag{34}$$

Thus to a good accuracy equation (34) for $r \gg 1$ agrees with relation (31) obtained by neglecting the radial part of the Laplacian operator.

Let us now match the near-field and far-field expansions. As it is seen from equation (26) the function $\epsilon_0(r)$ has a maximum at $r = r_c \equiv 8^{1/2} (3\tau)^{-1/2}$. Therefore, it seems reasonable to use this point as a matching point. From equation (31) we obtain that for $r = r_c, m_c = 4\tau^{1/2} r_c^2 / 3$, and for $\tau \gg 1, m_c \ll 1$. Therefore for $r = r_c$, the amplitude function in the far field (33) can be approximately presented as

$$\epsilon(r, \chi) \approx \sqrt{\tau} - \frac{1}{2} \cos(3\chi). \tag{35}$$

In the same way, the phase function in the far field (30) can be presented as

$$\Phi(r, \chi) \approx \chi + \frac{m_c}{12} \sin(3\chi). \tag{36}$$

Comparing equation (35) and equation (26), we obtain that

$$a_1 \approx \frac{3\sqrt{3}}{4\sqrt{2}} \tau, \quad a_2 \approx -\frac{9}{128} \tau^2. \tag{37}$$

Inserting now equation (37) into equation (25) and comparing the result for $\psi_1(r_c)$ with the result with the corresponding coefficient in equation (36), we see that their relative difference

$$\left(\psi_1(r_c) - \frac{m_c}{12} \right) / \left(\psi_1(r_c) + \frac{m_c}{12} \right) < 10^{-1},$$

which is quite reasonable when it is considered that we used only the first two terms in the near-field expansion (26).

Figure 2 represents the phase Φ from equation (32) and the components of the vector $(\cos \Phi, \sin \Phi)$ for two different distances from the centre of the vortex. Figures 3 and 4 represent the corresponding vector fields. Thus, the textured-vortex solution given by equations (30) and (33) describes three co-existing phases. Near-field configurations have a clear vortex (antivortex) structure which does not differ significantly from the no-third-order-nonlinearity case when $\Phi = \pm \chi$. However, in the long-distance limit the role of the third-order nonlinearity is crucial. Due to the existence of this term the two-dimensional space is divided into three domains (variants). Each pair of variant phases is separated by a semi-infinite domain wall which emanates from the centre of the structure. Figure 5 shows the χ dependence of the quantity $\epsilon = \sqrt{\phi_1^2 + \phi_2^2}$ for $r = 6$. Note that the far-field behaviour of the amplitude function $\epsilon(r, \chi)$ (see figure 5) is similar to cnoidal dark solitons in the nonlinear Schrödinger model.

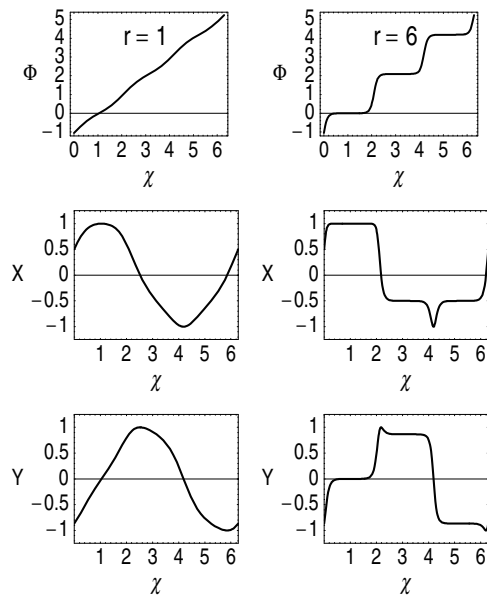


Figure 2. The azimuthal angle Φ and the vector-field components $(X, Y) = (\cos \Phi, \sin \Phi)$ for the three-domain wall junction structures, as functions of the polar angle χ (in rad). The left column corresponds to the distance $r = 1$ from the junction; the right column corresponds to $r = 6$.

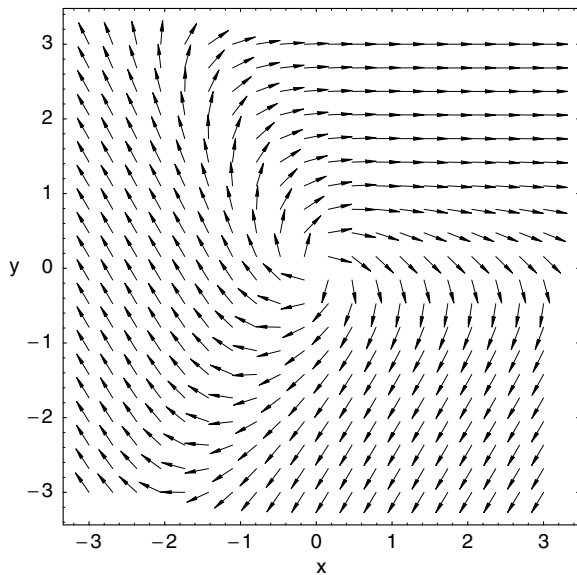


Figure 3. Vector-field distribution (in Cartesian coordinates) for the three-domain wall junction with the topological charge equal to 1.

We conclude that our interpolating functions seemed to work quite well and this will be further investigated in a subsequent paper where we study numerical and dynamical effects. To summarize, we have found analytic solutions for domain wall and Y-junction topological

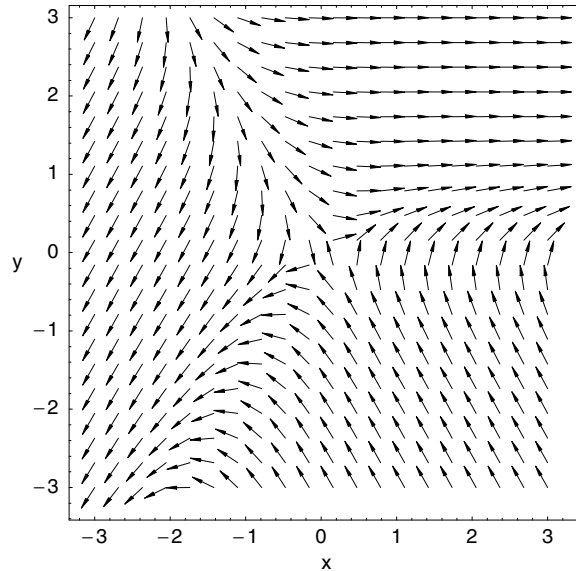


Figure 4. Vector-field distribution for the three-domain wall junction with the topological charge equal to -1 .

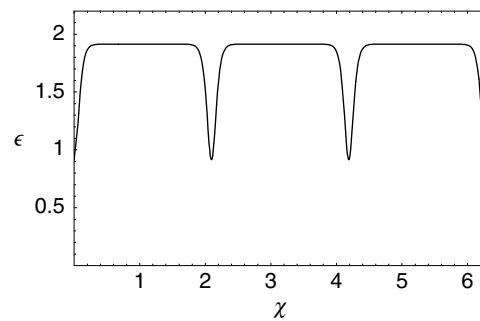


Figure 5. The variation of the modulus of the complex scalar field $\epsilon = |\phi|$ for the case of a three-domain wall junction.

defects in a two-component field theory with three-fold rotation symmetry. These results are of general interest in solid state physics, high energy physics and many other physical contexts.

Acknowledgments

YuBG is grateful for the hospitality of the Los Alamos National Laboratory and the University of Bayreuth where this work was performed. YuBG acknowledges support from Deutsches Zentrum für Luft- und Raumfahrt e.V., Internationales Büro des Bundesministeriums für Forschung und Technologie, Bonn, in the frame of a bilateral scientific cooperation between Ukraine and Germany, project no UKR-02/011. Work at Los Alamos is performed under the auspices of the US Department of Energy.

Appendix A

Let us consider the domain walls when the temperature τ deviates from the special case value: $\tau = 2 - \delta$, where $|\delta| < 1$. We study the case when the domain wall which separates the two variants is parallel to the y -axis. In this case, the Euler–Lagrange equations (12) take the form

$$\begin{aligned} -\partial_x^2 \phi_2 - \tau \phi_2 + 2\phi_1 \phi_2 + (\phi_1^2 + \phi_2^2) \phi_2 &= 0, \\ -\partial_x^2 \phi_1 - \tau \phi_1 + \phi_2^2 - \phi_1^2 + (\phi_1^2 + \phi_2^2) \phi_1 &= 0. \end{aligned} \quad (\text{A1})$$

It is more convenient to re-normalize our set of variables:

$$\phi_2(x) = \frac{\sqrt{3}}{4}(1 + \sqrt{1 + 4\tau})g_2(x), \quad \phi_1(x) = -\frac{1 + \sqrt{1 + 4\tau}}{4} + g_1(x). \quad (\text{A2})$$

The new variables g_1, g_2 for all values of δ satisfy the boundary conditions

$$g_2(x) \rightarrow \pm 1, \quad g_1 \rightarrow 0 \quad \text{when } x \rightarrow \pm\infty. \quad (\text{A3})$$

It is clear that for small δ the function $g_1(x)$ is also small. Introducing the new variables (A2) into equations (A1) and expanding them in a series with respect to δ and $g_1(x)$, we obtain

$$\partial_x^2 g_2 + (3 - \delta)g_2(1 - g_2^2) = 0, \quad (\text{A4})$$

$$\partial_x^2 g_1 - 3(1 + g_2^2)g_1 + \frac{\delta}{2}(1 - g_2^2) = 0, \quad (\text{A5})$$

where the terms $\delta^n g_2^m$ with $n + m \geq 2$ have been omitted. The solution of equation (A4) which satisfies the boundary condition (A3) has the form

$$g_2(x) = \tanh\left(\sqrt{\frac{3 - \delta}{2}}x\right). \quad (\text{A6})$$

In the temperature interval $|\tau + 2| \equiv |\delta| < 1$ the equation for $g_1(y)$, after rescaling the spatial variable $x = \sqrt{\frac{2}{3 - \delta}}z$, has the form

$$-\frac{d^2}{dz^2}g_1 - \frac{6}{3 - \delta} \frac{1}{\cosh^2 z} g_1 + \frac{12}{3 - \delta} g_1 - \frac{\delta}{3 - \delta} \frac{1}{\cosh^2 z} = 0. \quad (\text{A7})$$

Let us consider the eigenvalue problem

$$-\psi'' - U(z)\psi = \lambda\psi, \quad U = -\frac{6}{3 - \delta} \operatorname{sech}^2(z). \quad (\text{A8})$$

It is well known [42] that the number of discrete levels in the potential U in equation (A8) is equal to the largest integer satisfying the inequality

$$N < \frac{1}{2} \left(\sqrt{\frac{24}{3 - \delta} + 1} - 1 \right). \quad (\text{A9})$$

When $\delta = 0$ there is only one discrete level $\lambda = -1$ and the second level appears when $\delta \geq 2$. Therefore, for all $\delta < 2$ there is only one discrete level in the potential U . Note that the condition for the appearance of the second level coincides with the condition that the point $\phi_1 = \phi_2 = 0$ becomes a saddle point ($\tau = 0$). Thus, restricting ourselves to the case of small δ , we can safely neglect it in the potential U . (The eigenfunctions and eigenvalues do not change qualitatively in this case.) When $\delta = 0$ equation (A8) has the following set of eigenfunctions and eigenvalues:

$$\begin{aligned} \psi &= \frac{\sqrt{2}}{\operatorname{sech} z}, & \lambda &= -1, \\ \psi_k &= \frac{1}{\sqrt{2\pi}} \frac{\tanh z - ik}{1 - ik} e^{ikz}, & \lambda_k &= k^2 \quad (-\infty < k < \infty). \end{aligned} \quad (\text{A10})$$

In the same approximation, equation (A5) can be written as

$$-\frac{d^2}{dz^2}g_1 - \frac{2}{\cosh^2 z}g_1 + 4g_1 - \frac{\delta}{3} \frac{1}{\cosh^2 z} = 0. \tag{A11}$$

Using the eigenfunction expansion of the function g_2

$$g_2 = a\psi + \int_{-\infty}^{\infty} a_k \psi_k dk, \tag{A12}$$

and introducing it in equation (A11), we obtain

$$a = \frac{\pi\delta}{18\sqrt{2}}, \quad a_k = \frac{\delta}{6} \sqrt{\frac{\pi}{2}} \frac{ik^2}{(k^2+4)(k^2+1)} \frac{1}{\sinh\left(\frac{k\pi}{2}\right)}. \tag{A13}$$

Inserting the coefficients (A13) into the expansion (A12) and calculating corresponding integrals, we obtain the expression for the function g_1 in the form

$$g_1 = \frac{\delta}{18} (-1 + 4 \cosh^2 z \ln(2 \cosh z) - 2z(1 + 2 \cosh^2 z) \tanh z). \tag{A14}$$

Appendix B

The aim of this appendix is to check the accuracy of the solution given by equations (30) and (31). We have used the fact that equation (28) is the Euler–Lagrange equation for the functional

$$F_{sg} = \frac{1}{2} \int_0^\infty d\rho \int_0^{2\pi} d\chi \rho \left\{ (\partial_\rho \Phi)^2 + \frac{1}{\rho^2} (\partial_\chi \Phi)^2 + \frac{2}{3} (1 - \cos(3\Phi)) \right\}, \tag{B1}$$

with $\rho = \tau^{1/4}r$, and as a second step of our procedure we used equation (32) as a trial function for the functional (B1) with the modulus $m(\rho)$ being a collective variable which is to be determined. By introducing equation (32) into equation (B1) and carrying out an integration over the variable χ we obtain

$$F_{sg-v} = \pi \int_0^\infty d\rho \rho \left\{ \frac{1}{2} L^2(m) \left(\frac{dm}{d\rho} \right)^2 + U(\rho, m) \right\}, \tag{B2}$$

where $L(m)$ is an effective radial dispersion length given by

$$L^2(m) = \frac{2}{9m^2(1-m)^2\mathbf{K}} \int_0^{\mathbf{K}} du (Z(u|m) - m \operatorname{sn}(u|m) \operatorname{cd}(u|m))^2 \operatorname{dn}^2(u|m), \tag{B3}$$

and

$$U(\rho, m) = \frac{4}{\pi^2 \rho^2} \mathbf{E}\mathbf{K} + \frac{4}{3} \frac{\mathbf{E} - (1-m)\mathbf{K}}{m\mathbf{K}} \tag{B4}$$

is an effective potential. In equations (B3) and (B4) $pq(u|m)$ ($p, q = d, c, n, s$) are Jacobi elliptic functions and $Z(u|m)$ is Jacobi’s Zeta function; \mathbf{K} and \mathbf{E} are complete elliptic integrals of first and second kind, respectively [40].

Taking into account the definition of Jacobi’s Zeta function [40]

$$Z(u|m) = E(u|m) - u \frac{\mathbf{E}}{\mathbf{K}}, \tag{B5}$$

where $E(u|m)$ is the incomplete elliptic integral of the second kind:

$$\frac{d}{du} E(u|m) = \operatorname{dn}^2(u|m), \tag{B6}$$

and carrying out a few integrations by part, we get

$$L^2 = \frac{1}{m^2(1-m)^2} \frac{2\mathbf{E}}{9\mathbf{K}} (T_1 + T_2), \quad (\text{B7})$$

$$T_1 = \frac{\mathbf{E}}{\mathbf{K}} - \frac{2-m}{3} - \frac{1-m}{3} \frac{\mathbf{K}}{\mathbf{E}}, \quad (\text{B8})$$

$$T_2 = \frac{1}{\mathbf{K}} \int_0^{\mathbf{K}} \mathbf{Z}^2(u|m) du = \frac{\pi^2}{2\mathbf{K}^2} \sum_{n=1}^{\infty} \frac{1}{\sinh^2(n\xi)}, \quad \xi \equiv \ln q = \pi \frac{\mathbf{K}'}{\mathbf{K}}. \quad (\text{B9})$$

Here the q series for Jacobi's Zeta function [40] was used. To evaluate the sum in equation (B9) we use the relation between Weierstrass' ζ and \wp functions and Jacobi's θ_1 function [41]

$$\zeta(2\omega v) = 2\zeta(\omega)v + \frac{1}{2\omega} \frac{d}{dv} \ln \theta_1(v), \quad (\text{B10})$$

$$-2\omega\wp(2\omega v) = 2\zeta(\omega) + \frac{1}{2\omega} \frac{d^2}{dv^2} \ln \theta_1(v),$$

where 2ω is the real primitive period. Combining equation (B10) with the equation [41]

$$\theta_1(v) = 2q^{1/4} \sin \pi v \prod_{n=1}^{\infty} (1 - q^n)(1 - 2q^{2n} \cos 2\pi v + q^{4n}), \quad (\text{B11})$$

we get

$$-4\omega^2\wp(2\omega v) = 4\omega\zeta(\omega) + \pi^2 \sum_{n=-\infty}^{\infty} \frac{1}{\sinh^2(n\xi + in v)}. \quad (\text{B12})$$

Then in the limit $v \rightarrow 0$ from equation (B12) we obtain

$$\sum_{n=1}^{\infty} \frac{1}{\sinh^2 n\xi} = \frac{1}{6} - \frac{2}{\pi^2} \omega\zeta(\omega) = \frac{1}{6} \left(1 + \frac{\theta_1'''(0)}{\pi^2 \theta_1'(0)} \right), \quad (\text{B13})$$

where the relation [41]

$$\zeta(\omega) = -\frac{1}{12\omega} \frac{\theta_1'''(0)}{\theta_1'(0)}$$

was used. Inserting equations (B13) into equation (B9) yields

$$L^2(m) = \frac{1}{m^2(1-m)^2} \frac{2}{9\mathbf{K}} \left(\frac{\mathbf{E}^2}{\mathbf{K}} - \frac{2-m}{3} \mathbf{E} - \frac{1-m}{3} \mathbf{K} + \frac{\pi^2 \mathbf{E}}{12\mathbf{K}^2} \left(1 + \frac{\theta_1'''(0)}{\pi^2 \theta_1'(0)} \right) \right). \quad (\text{B14})$$

It is worth noting, however, that this expression, despite being exact, is not so useful. Since we are mostly interested in the asymptotic $m \rightarrow 1$ behaviour, we derive an approximate expression for the function (B9). In the limit $m \rightarrow 1$, $\xi \rightarrow 0$ and the function $1/\sinh^2 n\xi$ has a double pole. By applying the regularization procedure

$$\sum_{n=1}^{\infty} \frac{1}{\sinh^2 n\xi} = \sum_{n=1}^{\infty} \frac{1}{n^2 \xi^2} + \sum_{n=1}^{\infty} \left(\frac{1}{\sinh^2 n\xi} - \frac{1}{n^2 \xi^2} \right) \quad (\text{B15})$$

we may use the Euler–Maclaurin summation formula [40] for the second sum in equation (B15) and get

$$\begin{aligned} \sum_{n=1}^{\infty} \frac{1}{\sinh^2 n\xi} &= \frac{\pi^2}{6\xi^2} + \int_0^{\infty} dn \left(\frac{1}{\sinh^2 n\xi} - \frac{1}{n^2 \xi^2} \right) \\ &\quad - \frac{1}{2} \left(\frac{1}{\sinh^2 n\xi} - \frac{1}{n^2 \xi^2} \right) \Big|_{n \rightarrow 0} = \frac{\pi^2}{6\xi^2} - \frac{1}{\xi} + \frac{1}{6}. \end{aligned} \quad (\text{B16})$$

Inserting equation (B16) into equation (B9) we obtain

$$T_2 = \frac{\pi^2}{12\mathbf{K}^2} - \frac{\pi}{2\mathbf{K}\mathbf{K}'} + \frac{\pi}{12\mathbf{K}^2}. \quad (\text{B17})$$

Combining equations (B8), (B17) and (B7) we obtain the following expression for the effective dispersion length $L^2(m)$:

$$L^2(m) = \frac{2}{9m^2(1-m)^2} \frac{\mathbf{E}}{\mathbf{K}} \left(\frac{\pi^2}{12\mathbf{K}^2} - \frac{\mathbf{E}'}{\mathbf{K}'} + \frac{1+m}{3} + \frac{\pi^2}{12\mathbf{K}^2} - \frac{1-m}{3} \frac{\mathbf{K}}{\mathbf{E}} \right). \quad (\text{B18})$$

This approximate dispersion length agrees very well with the exact one for $m \geq 0.7$. In the limit $m \rightarrow 1$ when $\mathbf{K} \approx 0.5 \ln(16/(1-m))$, equation (B18) reduces to

$$L^2(m) = \frac{\pi^2}{54m^2(1-m)^2} (\mathbf{K}^{-3} + \mathcal{O}(1-m)). \quad (\text{B19})$$

The Euler–Lagrange equation for the function $m(\rho)$ is

$$-\frac{1}{\rho} \frac{d}{d\rho} \left(\rho L^2(m) \frac{dm}{d\rho} \right) + L \frac{dL}{dm} \left(\frac{dm}{d\rho} \right)^2 + \frac{\partial U}{\partial m} = 0. \quad (\text{B20})$$

For large r when $(1-m) \ll 1$, we obtain from equation (B20) that the function $\mathbf{K}(m)$ satisfies the equation

$$\frac{1}{\rho} \frac{d}{d\rho} \left(\frac{\rho}{\mathbf{K}^3} \frac{d\mathbf{K}}{d\rho} \right) + \frac{3}{2\mathbf{K}^4} \left(\frac{d\mathbf{K}}{d\rho} \right)^2 - \frac{18}{\pi^2} \left(\frac{3}{\pi^2 \rho^2} - \frac{1}{\mathbf{K}^2} \right) = 0. \quad (\text{B21})$$

It is straightforward to see that the asymptotic behaviour of the function $Q = 1/\mathbf{K}^2$ is given by

$$Q = \frac{3}{\pi^2 \rho^2} + \frac{1}{12\rho^4} + \mathcal{O}(\rho^{-6}), \quad \mathbf{K} \approx \frac{\pi\rho}{\sqrt{3}} \left(1 + \frac{\pi^2}{36\rho^2} \right)^{-1/2}. \quad (\text{B22})$$

Thus, with a good accuracy equation (B22) for $r \gg 1$ agrees with relation (31) obtained by neglecting the radial part of the Laplacian operator.

References

- [1] Jaffe A and Taubes C 1980 *Vortices and Monopoles: Structure of Static Gauge Theories* (Boston: Birkhauser)
- [2] Vilenkin A and Shellard E P S 1994 *Cosmic Strings and Other Topological Defects* (Cambridge: Cambridge University Press)
- [3] de Gennes P G 1974 *The Physics of Liquid Crystals* (Oxford: Clarendon)
- [4] Nelson D R 1983 *Phase Transitions and Critical Phenomena* vol 7, ed C Domb and J L Lebowitz (London: Academic)
- [5] Sasa S 1992 *Phys. Rev. A* **46** 5268
- [6] Sternberg P and Zeimer W P 1994 *Proc. R. Soc. Edinburgh A* **124** 1059
- [7] Nielsen H B and Olesen P 1973 *Nucl. Phys. B* **61** 45
- [8] Trappenberg T and Wiese U J 1992 *Nucl. Phys. B* **372** 703
- [9] Smilga A V and Veselov A I 1997 *Phys. Rev. Lett.* **79** 4529
- [10] Kogan I I, Kovner A and Shifman M 1998 *Phys. Rev. D* **57** 5195
- [11] Carroll S M and Trodden M 1998 *Phys. Rev. D* **58** 5189
- [12] Smilga A V 1998 *Phys. Rev. D* **58** 065005
- [13] Carroll S M, Hellerman S and Trodden M 2000 *Phys. Rev. D* **61** 065001
- [14] Vilenkin A 1994 *Phys. Rev. Lett.* **72** 3137
- [15] Linde A 1994 *Phys. Lett. B* **327** 208
- [16] Yu R P, Adam N, Thatcher M J and Morgan M J 2001 *Class. Quantum Grav.* **18** L163
- [17] Yu R P and Morgan M J 2002 *Class. Quantum Grav.* **19** L157
- [18] Silverman M P and Malett R L 2001 *Class. Quantum Grav.* **18** L103

- [19] Axenides M, Perivolaropoulos L and Trodden M 1998 *Phys. Rev. D* **58** 083505
- [20] Gopalan V, Gerstl S S A, Itagi A, Mitchell T E, Jia Q X, Schlesinger T E and Stancil D D 1999 *J. Appl. Phys.* **86** 1638
- [21] Curnoe S H and Jacobs A A 2001 *Phys. Rev. B* **63** 094110
- [22] Lookman T, Shenoy S R, Rasmussen K Ø, Saxena A and Bishop A R 2003 *Phys. Rev. B* **67** 024114
- [23] Bodenschatz E, Pesch W and Kramer L 1988 *Physica D* **32** 135
- [24] Soskin M S and Vasnetsov M V 2001 *Singular optics Progr. Opt.* **42** 219
- [25] Matthews M R, Anderson B P, Haljan P C, Hall D S, Wieman C E and Cornell E A 1999 *Phys. Rev. Lett.* **83** 2098
Haljan P C, Coddington I, Engels P and Cornell E A 2001 *Phys. Rev. Lett.* **87** 210403
- [26] Pulwey R, Rahm M, Biberger J and Weiss D 2001 *IEEE Trans. Magn.* **37** 2076
- [27] Wachowiak A, Wiebe J, Bode M, Pietzsch O, Morgenstern M and Wiesendanger R 2002 *Science* **298** 577
- [28] Borisov A B and Kiseliev V V 1988 *Physica D* **31** 49
Borisov A B and Kiseliev V V 1988 *Physica D* **111** 96
- [29] Chui S T and Ryzhov V N 1997 *Phys. Rev. Lett.* **78** 2224
- [30] Castro J, Chui S T and Ryzhov V N 1999 *Phys. Rev. B* **60** 10271
- [31] Landau L D and Lifshitz E M 1959 *Statistical Physics* (London: Pergamon)
- [32] Polyakov A M 1977 *Nucl. Phys. B* **120** 429
- [33] 't Hooft G 1978 *Nucl. Phys. B* **138** 1
- [34] Ruck H M 1980 *Nucl. Phys.* **167** 320
- [35] Curnoe S H and Jacobs A E 2001 *Phys. Rev. B* **62** R11 925
- [36] Rasmussen K Ø, Lookman T, Saxena A, Bishop A R, Albers R C and Shenoy S R 2001 *Phys. Rev. Lett.* **87** 055704-1
- [37] Campos A, Holland K and Wiese U-J 1998 *Phys. Rev. Lett.* **81** 2420
- [38] Mazor A and Bishop A R 1989 *Physica D* **39** 22
- [39] Bronsard L and Reitich F 1993 *Arch. Ration. Mech. Anal.* **124** 355
- [40] Abramowitz M and Stegun I 1972 *Handbook of Mathematical Functions* (New York: Dover)
- [41] Bateman H and Erdélyi A 1953 *Higher Transcendental Functions* vol 2 (New York: McGraw-Hill)
- [42] Landau L D and Lifshitz E M 1965 *Quantum Mechanics* (Oxford: Pergamon)
- [43] Takeno S 1982 *Progr. Theor. Phys.* **68** 992